Influence of Plasma Reactor Structure on Methanol Oxidation

S. Yao, X. Zhang, and B. Lu
School of Environment Science and Technology, Tianjin University, Tianjin 300072, China

DOI 10.1002/aic.10450
Published online March 28, 2005 in Wiley InterScience (www.interscience.wiley.com).

Plasma oxidation of methanol (CH_3OH) in oxygen and nitrogen was investigated using two dielectric barrier discharge (DBD) reactors with or without Al_2O_3 as a catalyst and using a DC circle-to-plate (CTP) reactor. An AC power supply was used for the DBD reactors to generate corona discharges. A DC power supply, a 20-MΩ resistor, and a 100-pF capacitor were used to yield pulselike discharges. CH_3OH was oxidized to formaldehyde (HCHO), carbon monoxide (CO), and carbon dioxide (CO_2). HCHO was the main product when using DBD reactors and without Al_2O_3. CO was the main product when using the DBD reactor with Al_2O_3 and CTP reactor. Al_2O_3 could inhibit CH_3OH further oxidation. The energy efficiency of the DBD reactors decreased with increasing power input and power density. The energy efficiency of the CTP reactor peaked with 7 g CH_3OH/kWh that was three times as high as that with the DBD reactors at the same power input. Furthermore, the power density of the CTP reactor was higher than that of the DBD reactors, implying that the CTP reactor could be used for CH_3OH oxidation with a small discharge space volume. *AIChE J,* 51: 1558–1564, 2005
Keywords: methanol oxidation, corona discharges, spark discharges

Introduction

The abatement technologies for controlling hazardous air pollutants, such as volatile organic compounds (VOCs), are becoming increasingly important with respect to consideration of human health and globe warming. In particular, emission of VOCs from building materials and indoor furniture in China has been the focus of increased attention. To reduce emission of VOCs, thermal incineration with or without catalysts, adsorption, condensation, biofiltration, membrane separation, ultraviolet (UV) oxidation, and plasma discharge have become the center of a number of investigations. In 1997 Vercammen et al.[1] reported that plasma discharge technologies are useful for reducing VOCs at gas flow rates < 1000 Nm^3/h and concentrations $< 10\%$. Many types of plasma discharges have been developed, among which corona discharges are of interest because this kind of plasma can be carried at ambient temperature and atmospheric pressure, and at an operation cost lower than that of thermal incineration.[2-17] However, plasma discharge technologies have encountered site-specific constraints (such as economic considerations) that have limited their commercial availability.[18]

Recently, one of the authors developed a pulsed-plasma discharge for methane conversion using a point-to-point (PTP) reactor and diesel particulate matter (PM) removal using a dielectric barrier discharge (DBD) reactor, which implied that the energy efficiency of the plasma discharges is related to the structure of the reactor. For methane conversion, acetylene is the main product conventionally produced by hydrocarbon partial oxidation at an elevated temperature and followed by rapid quenching. The pulsed-plasma discharge with a PTP reactor is a rapid heating process, with a peak power density of about 10^9 watts per liter (W/L) of discharge space and rapid cooling, suggesting that the pulsed-plasma discharge with the PTP reactor is suitable for conversion of methane to acetylene.[19,20] For

Correspondence concerning this article should be addressed to S. Yao at yao@rite.or.jp.

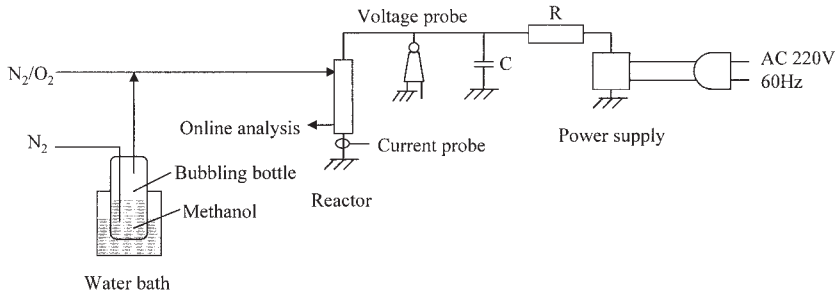

Figure 1. Plasma system for the plasma oxidation of methanol.

PM removal by carbon oxidation, DBD reactors driven by a pulsed-power supply (to treat a large amount of gaseous exhausts from diesel engines) have a peak power density of 10^4 W/L of discharge space.[21,22] The types of plasma reactors and power supplies may influence the energy efficiency of removal of VOCs from a limited space. In this study, three types of reactors were used for methanol decomposition (oxidation), using AC and DC power supplies at room temperature and atmospheric pressure. The mechanism of methanol oxidation in plasmas was suggested.

Experimental Setup

Figure 1 shows the experimental systems, which include three gas flow meters, a CH_3OH bubbling bottle, a plasma reactor, and a power supply unit. The CH_3OH bubbling bottle was held in a 25°C water bath to obtain a certain gaseous CH_3OH concentration. A gas mixture of N_2, O_2, and CH_3OH was used. N_2 was supplied at a rate of 77.3 mL/min, in which 8.76 mL/min was used for methanol bubbling. O_2 was supplied at a rate of 21.3 mL/min. CH_3OH concentration in the gas mixture was estimated to be 1.81%. A direct current (DC) power supply and an alternating current (AC) power supply were used. The AC power supply was used for dielectric barrier discharge (DBD) reactors. The DC power supply and a high-voltage capacitor (100 pF) and resistor (20 MΩ) were used to generate a pulselike discharge by the self-breakdown of the discharge gap. The output powers P of the power supplies were calculated from the average output voltage meters and average output current meters equipped on DC and AC power supplies.

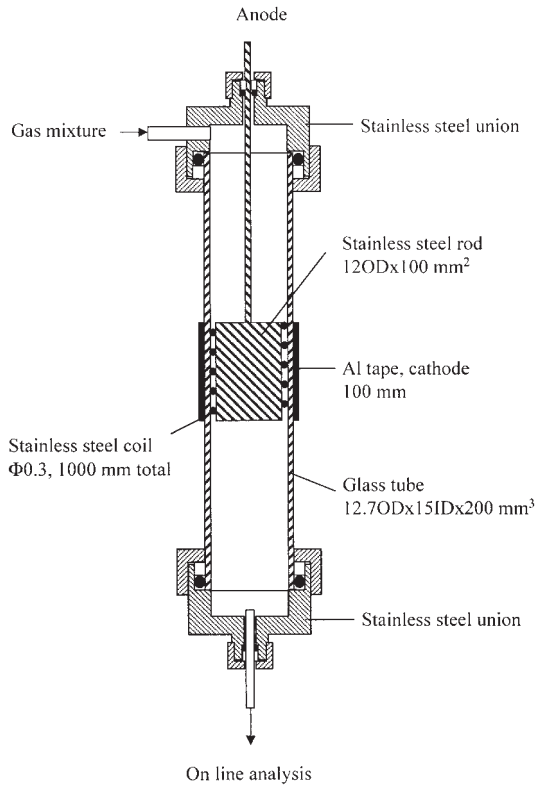

Figure 2. Structure of DBD reactor (DBD1).

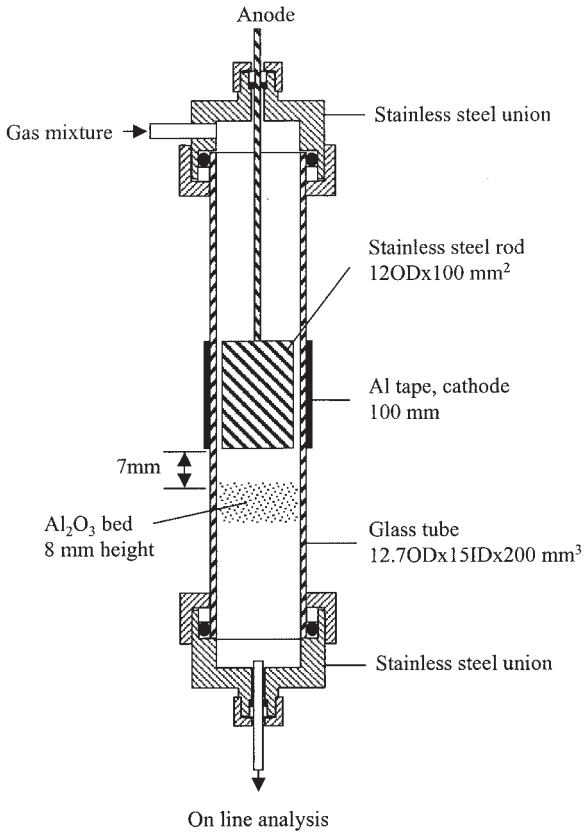

Figure 3. Structure of DBD reactor (DBD2) with Al_2O_3.

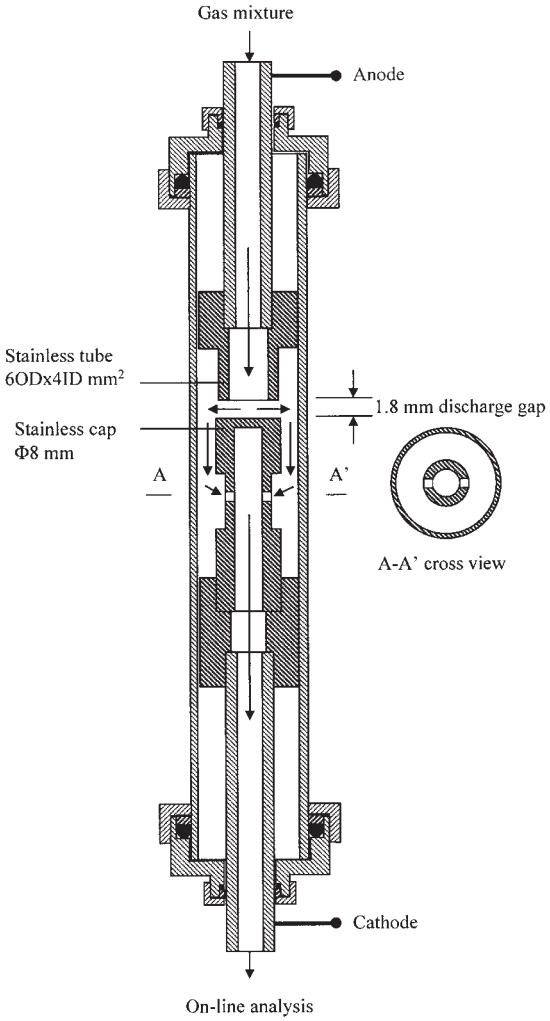

Figure 4. Structure of CTP reactor.

Power densities P_V and P_F are defined in Eqs. 1 and 2 in W/mL of discharge space volume (V_R) or in joules per liter of the gas mixture, respectively

$$P_V = \frac{P}{V_R} \qquad [\text{W/mL}] \tag{1}$$

$$P_F = \frac{P}{F} \qquad [\text{W/L}] \tag{2}$$

where F is the flow rate of the gas mixture in L/s.

Three types of reactors are illustrated in Figures 2–4, in which corona discharges or pulsed-spark discharges occur. Two DBD reactors (Figures 2 and 3) primarily consist of a glass tube inserted between anode and cathode. The discharge zone is limited in the space between the outside surface of the coil and the inside surface of the glass tube in the DBD1 reactor (Figure 2) and in the space between the outside surface of the stainless steel rod and the inside surface of the glass tube in the DBD2 reactor (Figure 3). A 1.04-g sample of α-Al_2O_3 particles was filled 7 mm beneath the stainless rod with an 8-mm bed height in the DBD2 reactor (Figure 3). The properties of α-Al_2O_3 particles are as follows: sphere diameter, 2 to 4 mm; surface area, 6.9 m^2/g (BET); hole volume, 3.8×10^{-4} L/g; fill density, 980 g/L. A circle-to-plate (CTP) reactor was mainly made from a stainless steel tube and stainless steel cap (Figure 4). The discharge zone in the CTP reactor was the space between the side cross surface of the stainless tube and the top surface of the stainless cap. The main factors and discharge conditions for each reactor are listed in Table 1.

The discharge voltage and cathode discharge current were measured with a voltage probe (P6015A, Tektronix) and a current transformer (TCP202, Tektronix), respectively. The analogue signals from the voltage probe and current transformer were recorded with a digital phosphor oscilloscope (TDS3054B, Tektronix).

All experiments were carried out at atmospheric pressure and without external heating, except plasma heating.

CH_3OH and its oxidation products were analyzed online with a gas chromatograph (SP-3430, BFRL, Beijing, China), equipped with a 2-m Porapak-N and a methanizer, before analysis by flame ionization detector. CH_3OH conversion was calculated using Eq. 3. Carbon products of formaldehyde (HCHO), carbon monoxide (CO), and carbon dioxide (CO_2) were found in this study. The carbon balance was >95%. The selectivity of each carbon product was calculated using Eq. 4.

$$CH_3OH \text{ conversion} = \frac{CH_3OH \text{ concentration without plasmas} - CH_3OH \text{ concentration with plasmas}}{CH_3OH \text{ concentration without plasmas}} \times 100\% \tag{3}$$

Table 1. Main Factors and Discharge Conditions for Each Reactor

Reactor Type	Discharge Type	Reactor Volume (mL)	Residence Time (s)	Power Supply	R (MΩ)	C (pF)
DBD1	Corona	1.35	0.81	AC	None	None
DBD2	Corona	0.78	0.468	AC	None	None
CTP	Spark	0.028	0.0168	DC	2	100

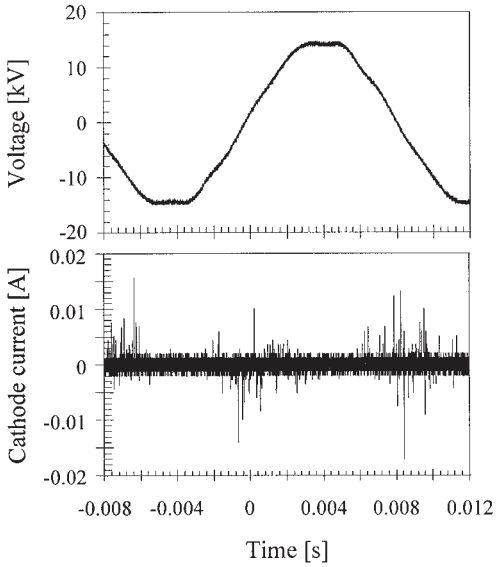

Figure 5. Waveforms of discharge voltage and cathode current using DBD2 reactor.

Selectivity of CO, CO_2, or HCHO

$$= \frac{\text{moles of CO, } CO_2\text{, or HCHO formed}}{\text{moles of } CH_3OH \text{ converted}} \times 100\% \quad (4)$$

The energy efficiency (in g CH_3OH/J and g CH_3OH/kWh) is defined as follows

$$\eta_d = \frac{\text{grams of } CH_3OH \text{ converted s}^{-1}}{P} \quad [\text{g/J}]$$

$$= \frac{\text{grams of } CH_3OH \text{ converted s}^{-1}}{P} \times 3.6 \times 10^6 \quad [\text{g/kWh}] \quad (5)$$

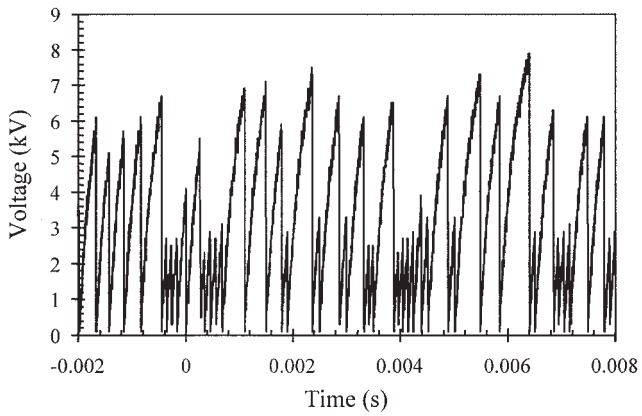

Figure 6. Voltage waveform using CTP reactor and DC power supply.

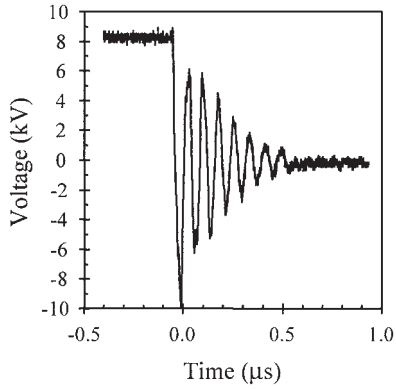

Figure 7. Voltage waveform in a pulselike discharge duration using CTP reactor and DC power supply.

Results and Discussion

Typical waveforms of discharge voltage and current

The typical waveforms of discharge voltage and cathode current, using the AC power supply and DBD2 reactor at an average out voltage and current of 10.4 kV and 0.9 mA, respectively, are shown in Figure 5. Although there was no obvious drop in voltage on the sine-wave form of voltage, there were multiple discharge current pulses that could be found from the waveform of discharge current. Those multiple discharge current pulses induce the formation of corona discharges in the space between the stainless steel rod and the glass tube.[11,23,24]

In contrast with the DBD reactors, the waveforms of discharge voltage and current using the CTP reactor and DC power supply, together with a 2-MΩ resistor and a 100-pF capacitor, are shown in Figures 6–8, respectively. The discharge gap was broken down at voltage < 8.2 kV, which resulted in multiple pulselike discharges within the discharge gap of the CTP reactor. The frequency of those multiple pulselike discharges was estimated to be 2 to 3 kHz (Figure 6). After the gap was broken down, a high-voltage oscillation (about 12 MHz) was found with a duration time of about 0.5 μs (Figure 7). The discharge current wave could be observed almost in the same time duration with a positive peak current of 8 A and negative peak current of -16 A (Figure 8).

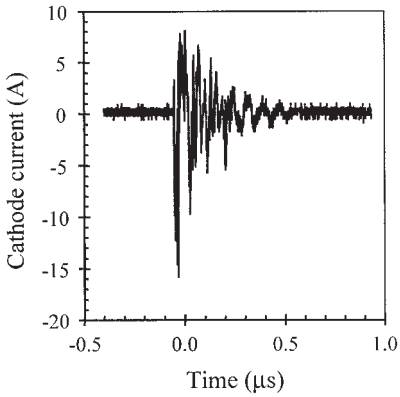

Figure 8. Cathode current waveform in a pulselike discharge duration using CTP reactor and DC power supply.

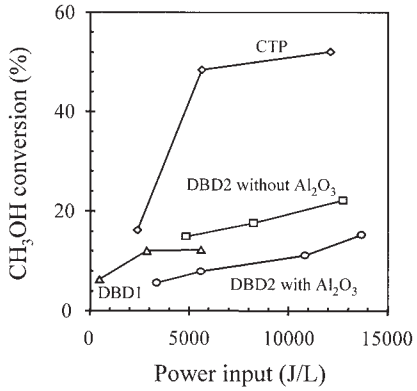

Figure 9. Methanol conversion as a function of power input using various types of reactors.

Methanol oxidation

The conversion of methanol is shown in Figure 9 as a function of power input. Methanol conversion increased with increasing power input. Methanol conversion using the CTP reactor was higher than that using either the DBD1 or the DBD2 reactor. Methanol conversion using the DBD2 reactor with Al_2O_3 was lowest compared with that using other kinds of reactors at the same power input. When the same DBD2 reactor was used, however, methanol conversion with Al_2O_3 was lower than that without Al_2O_3; this difference obviously results from the use of Al_2O_3. Al_2O_3 stopped methanol oxidation in the product stream gases from the discharge part of the DBD2 reactor.

The carbon products from CH_3OH oxidation in plasma discharges were found to be HCHO, CO, and CO_2. Figure 10 shows the selectivity of each product using the DBD1 reactor at various power inputs; at 8.1 W power input, HCHO selectivity was as high as 55.5%. With increasing power input, HCHO selectivity decreased and that of CO and CO_2 increased.

The selectivity of methanol oxidation products using the DBD2 reactor, with or without Al_2O_3, is shown in Figure 11. The selectivity of each product without Al_2O_3 was similar to that using the DBD1 reactor, having the following selectivity order: HCHO $>$ CO $>$ CO_2. However, the selectivity order

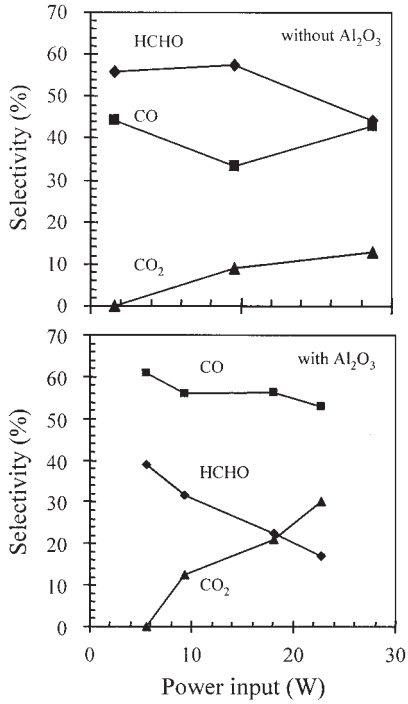

Figure 11. Selectivity of each product at various power inputs using DBD2 reactor and AC power supply with or without Al_2O_3.

with Al_2O_3 was CO $>$ HCHO $>$ CO_2 at a power input $<$ 18 W, and CO $>$ CO_2 $>$ HCHO at a power input $>$ 18 W.

The main product of methanol oxidation using the CTP reactor was CO and CO_2 at a power input $>$ 10 W (Figure 12).

Mechanism of methanol oxidation

The oxidation of methanol in plasma discharges would include the decomposition of methanol arising from the electron impact of electrons in the discharge zone and the oxidation of methanol in the space downstream from the discharge zone. The mechanism of methanol oxidation in a gas phase and over catalysts has been reported. The main reactions are listed in Eqs. 6–13.[25] The gaseous oxidation of CH_3OH starts with

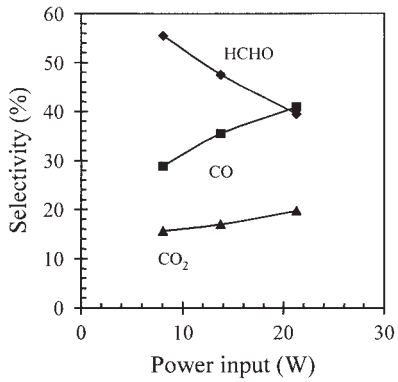

Figure 10. Selectivity of each product at various power inputs using DBD1 reactor and AC power supply.

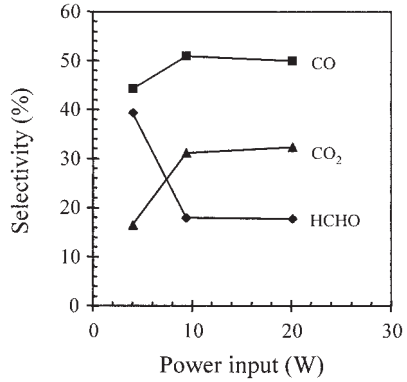

Figure 12. Selectivity of each product at various power inputs using CTP reactor and DC power supply.

dehydration by O and OH (Eqs. 6 and 7). O and OH also promote the oxidation of HCHO to CO_2 by HCO (Eqs. 9, 10, 12, and 13). CO formation is attributed to the reaction of HCO with O_2

$$CH_3OH + O = CH_2OH + OH \quad (6)$$

$$CH_3OH + OH = CH_2OH + H_2O \quad (7)$$

$$CH_2OH + O_2 = HCHO + HO_2 \quad (8)$$

$$HCHO + O = HCO + OH \quad (9)$$

$$HCHO + OH = HCO + H_2O \quad (10)$$

$$HCO + O_2 = HO_2 + CO \quad (11)$$

$$HCO + O = H + CO_2 \quad (12)$$

$$CO + OH = H + CO_2 \quad (13)$$

$$O_2 + e = 2O + e \quad (14)$$

$$O + O_2 = O_3 \quad (15)$$

$$O_3 + M = O_2 + O + M \quad (16)$$

$$O_3 + OH = O_2 + HO_2 \quad (17)$$

$$O_3 + HO_2 = OH + 2O_2 \quad (18)$$

In this study, O could be produced by plasma discharges (Eq. 14). The lifetime of O radicals [except the metastable state O (2^1D_2) with 110 s lifetime that could not form under the experimental conditions] is on the order of 10^{-5} to 10^{-4} s,[26] which implies that the O radicals disappeared as the gases flowed out from the discharge zone of the DBD1 and DBD2 reactors downstream to a distance $< 1.36 \times 10^{-3}$ mm. This phenomenon is explained by the facts that CH_3OH conversion without Al_2O_3 was higher than that with Al_2O_3 and that the residence time of the feed gas in the space between the discharge zone of the DBD2 reactor and Al_2O_3 was obviously longer than 10^{-4} s; thus CH_3OH oxidation in the downstream space is attributed not only to the O-radical–related reactions but also to the ozone (O_3)–related reactions.

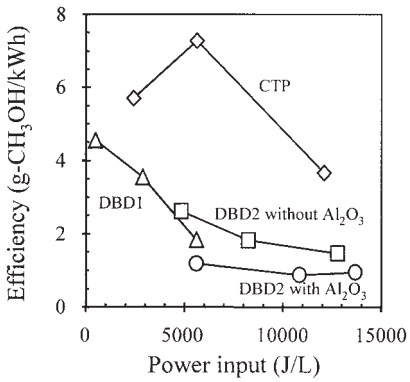

Figure 13. Energy efficiency as a function of power input using various types of reactors.

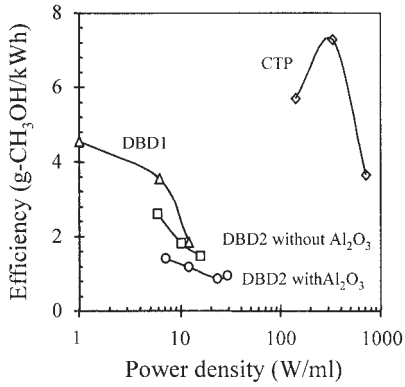

Figure 14. Energy efficiency as a function of power density using various types of reactors.

O_3 is formed from the combination of O and O_2 (Eq. 15). O_3 acted as a carrier to yield O and OH (Eqs. 16–18)[27]—both radicals play important parts in CH_3OH oxidation as described above.

Energy efficiency of methanol oxidation

The discharge energy efficiencies (η_d) of methanol oxidation at various power densities are illustrated in Figure 13. The CTP reactor had the highest energy efficiency, 1.5- to threefold that using the DBD1 reactor and the DBD2 reactor without Al_2O_3. The DBD2 reactor had the lowest energy efficiency as a result of the inhibition of gaseous CH_3OH oxidation with O_3. The discharge energy efficiency of methanol oxidation could also be illustrated as a function of power density (Figure 14). The CTP reactor had the highest energy efficiency and highest power density because of its smallest reaction volume. The energy efficiency using the DBD1 and DBD2 reactors decreased with increasing power density.

Conclusions

CH_3OH oxidation under plasma discharges and various types of reactors was investigated. CH_3OH oxidation is attributed not only to the O radicals but also, indirectly, to O from O_3 or directly by O_3.

Al_2O_3 could accelerate HCHO further oxidation, but inhibited CH_3OH oxidation. The energy efficiency with Al_2O_3 was lower than that without the use of Al_2O_3.

The CTP reactor had the highest energy efficiency and the main products were CO and CO_2. This type of reactor and the pulselike plasma discharges would be suitable for CH_3OH oxidation.

Literature Cited

1. Vercammen KLL, Berezin AA, Lox F, Chang JS. Non-thermal plasma techniques for the reduction of volatile organic compounds in air streams: A critical review. *J Adv Oxid Technol*. 1997;2:312-329.
2. Bromberg L, Cohn DR, Koch M, Patrick RM, Thomas P. Decomposition of dilute concentrations of carbon tetrachloride in air by an electron-beam generated plasma. *Phys Lett A*. 1993;173:293-299.

3. Chang JS, Lawless PA, Yamamoto T. Corona discharge processes. *IEEE Trans Plasma Sci*. 1991;19:1152-1166.
4. Dorai R, Hassouni K, Kushner MJ. Interaction between soot particles and NOx during dielectric barrier discharge plasma remediation of simulated diesel exhaust. *J Appl Phys*. 2000;88:6060-6071.
5. Eliasson B, Kogelschatz U. Nonequilibrium volume plasma chemical processing. *IEEE Trans Plasma Sci*. 1991;19:1063-1077.
6. Evans D, Rosocha LA, Anderson GK, Coogan JJ, Kushner MJ. Plasma remediation of trichloroethylene in silent discharge plasmas. *J Appl Phys*. 1993;74:5378-5386.
7. Koch M, Cohn DR, Patrick RM, Schuetze MP, Bromberg L, Reilly D, Thomas P. Electric field effects on decomposition of dilute concentrations of $CHCl_3$ and CCl_4 in electron beam generated air plasma. *Phys Lett A*. 1993;184:109-113.
8. Larkin DW, Caldwell TA, Lobban LL, Mallinson RG. Oxygen pathways and carbon dioxide utilization in methane partial oxidation in ambient temperature electric discharges. *Energy Fuels*. 1998;12:740-744.
9. Liu C, Mallinson RG, Lobban LL. Non-oxidative methane coupling to acetylene over zeolites in a low-temperature plasma. *J Catal*. 1998; 179:326-334.
10. Mizuno A, Kisanuki Y, Noguchi M, Katsura S, Lee SH, Hong YK, Shin SY, Kang JH. Indoor air cleaning using a pulsed discharge plasma. *IEEE Trans Ind Appl*. 1999;35:1284-1288.
11. Nunez CM, Ramsey GH, Ponder WH, Abbott JH, Hamel LE, Kariher PH. Corona destruction: An innovative control technology for VOCs and air toxics. *Air Wastes*. 1993;43:242-247.
12. Supat K, Kruapong A, Chavadej S, Lobban LL, Mallinson RG. Synthesis gas production from partial oxidation of methane with air in AC electric gas discharge. *Energy Fuels*. 2003;17:474-481.
13. Tamon H, Imanaka H, Sano N, Okazaki M, Tanthapanichakoon W. Removal of aromatic compounds in gas by electron attachment. *Ind Eng Chem Res*. 1998;37:2770-2774.
14. Tamon H, Mizota H, Sano N, Schulze S, Okazaki M. New concept of gas purification by electron attachment. *AIChE J*. 1995;41:1701-1711.
15. Tamon H, Sano N, Okazaki M. Influence of oxygen and water vapor on removal of sulfur compounds by electron attachment. *AIChE J*. 1996;42:1481-1486.
16. Thanyachotpaiboon K, Chavadej S, Caldwell TA, Lobban LL, Mallinson RG. Conversion of methane to higher hydrocarbons in AC nonequilibrium plasmas. *AIChE J*. 1998;44:2252-2257.
17. Yan K. *Corona Plasma Generation*. Eindhoven, The Netherlands: Technische Universititeit Eindhoven; 2001.
18. Moretti EC. Reduce VOC and HAP emissions. www.cepmagazine.org. *Chem Eng Prog* (CEP), AIChE. 2002;June.
19. Yao S, Nakayama A, Suzuki E. Methane conversion using a high-frequency pulsed plasma: Discharge features. *AIChE J*. 2001;47:419-426.
20. Yao S, Nakayama A, Suzuki E. Methane conversion using a high-frequency pulsed plasma: Important factors. *AIChE J*. 2001;47:413-418.
21. Yao S, Okumoto M, Shimogami J, Madokoro K, Yashima T, Suzuki E. Diesel particulate matter and NOx removals using a pulsed corona surface discharge. *AIChE J*. 2004;50:715-721.
22. Yao S, Okumoto M, Madokoro K, Yashima T, Suzuki E. A pulsed dielectric barrier discharge reactor for diesel particulate matter removal. *AIChE J*. 2004;50:1901-1907.
23. Yamamoto T, Ramanathan K, Lawless PA, Ensor DS, Newsome JR, Plaks N, Ramsey GH. Control of volatile organic compounds by an ac energized ferroelectric pellet reactor and a pulsed corona reactor. *IEEE Trans Ind Appl*. 1992;28:528-534.
24. Nozaki T, Unno Y, Miyazaki Y, Okazaki K. A clear distinction of plasma structure between APG and DBD. Vol. 1. Proc. of 15th International Symposium on Plasma Chemistry, Orleans, France; 2001:77-83.
25. Tsang W. Chemical kinetic data base for combustion chemistry. Part 2. Methanol, *J Phys Chem Ref Data*. 1987;16:471-508.
26. Chang JS, Hobson RM, Ichikawa Y, Kaneda T. *Process of Ionized Atoms and Molecules*. Tokyo, Japan: Tokyo Denki Univ. Press; 1989: 142.
27. Toby S, Toby FS. Reactivity of the ozone-ethane system. *J Phys Chem A*. 1998;102:4527-4531.

Manuscript received May 23, 2004, and revision received Sept. 27, 2004.